INL/EXT-08-15116

High Repetition Rate, LINAC-Based Nuclear Resonance Fluorescence FY 2008 Final Report

Mathew T. Kinlaw
James L. Jones
Scott M. Watson
Alan W. Hunt
Glen A. Warren

December 2008

The INL is a U.S. Department of Energy National Laboratory
operated by Battelle Energy Alliance

INL/EXT-08-15116

High Repetition Rate, LINAC-Based Nuclear Resonance Fluorescence FY 2008 Final Report

Mathew T. Kinlaw
James L. Jones
Scott M. Watson
Alan W. Hunt[1]
Glen A. Warren[2]

[1]Idaho State University
[2]Pacific Northwest National Laboratory

December 2008

Idaho National Laboratory
Idaho Falls, Idaho 83415

http://www.inl.gov

Prepared for the
U.S. Department of Energy
Office of National Nuclear Security Administration
Under DOE Idaho Operations Office
Contract DE-AC07-05ID14517

SUMMARY

The process of nuclear resonance fluorescence (NRF) can occur in all nuclei with atomic numbers (Z) greater than helium (Z=2). These nuclei have inherent nuclear states that can become populated following absorption of specific-energy photons. Nuclei excited to these unique and well-defined states, which exist in the several MeV range, will preferentially de-excite through the emission of discrete energy photons (fluorescence). By allowing a continuous energy photon spectrum, as is produced from bremsstrahlung radiation, to impinge upon a material of interest, excitation of the nuclei into the discrete energy states can be achieved. As these states decay either to the ground state or to a lower-energy excited state, the reemitted photons have specific energies corresponding to the energy difference between the excited state and the ground state (or lower-energy excited state). Because nuclear energy levels are unique from one isotope to another, the NRF states for an individual nucleus are also unique to that isotope. Therefore, the detection of photons from NRF provides unique, well-defined signatures of specific isotopes.

The Idaho National Laboratory's FY 2008 effort, in collaboration with the Idaho State University's Idaho Accelerator Center and Pacific Northwest National Laboratory, focused on an experimental assessment of NRF measurements using a pulsed linear electron accelerator (LINAC) with various repetition rates, including the identification of specific detection necessities/requirements for optimization of these measurements. The first task of FY 2008 identified an existing accelerator, located at the Idaho Accelerator Center, to rapidly support initial experimentation with a pulsed accelerator repetition rate up to 600 Hz. This nominal 25 MeV electron accelerator was originally designed with a maximum repetition rate up to 300 Hz. Hence, several modifications were made to the system, enabling the repetition rate to be increased to 600 Hz. These modifications involved reducing the overall capacitance and inductance of the pulse forming network (PFN) to provide a more rapid charging and discharging time and shortening the radio frequency driver pulse. The result of these modifications produced a total radio frequency pulse width of 3 μs. In support of increasing the system's repetition rate, the PFN charging power was increased to approximately 12 kW, which decreases total charging time. Typically, as much as half the power output from the PFN is passed into the accelerator's thyratron. With the increase of the PFN power to 12 kW, it was expected that the existing glass thyratron would be unable to properly operate with the increased power requirements. To accommodate such a power increase, the glass thyratron was replaced with a ceramic thyratron, which is more suitable for higher-power operation.

Following initial identification and modification of the up to 600 Hz LINAC operations, a series of preliminary experiments was performed (referred to as Phase I) to optimize the experimental setup for NRF-type testing, including baseline testing with non-nuclear materials. The nominal 25 MeV pulsed LINAC produced 5.3 and 3.3 MeV electrons, which interacted in a 4.2 g cm^{-2} tungsten converter to produce a 600 Hz pulsed bremsstrahlung beam. The targets tested included ^{nat}Pb (3.1 mm), ^{27}Al (25 mm), graphite (50 mm), and Borax (50 mm) irradiated with 5.3 MeV endpoint energy bremsstrahlung. Additional preliminary testing was performed with a depleted uranium target (25 mm) irradiated with 3.3 MeV endpoint energy bremsstrahlung. The NRF-produced photons were collected with a 62.1% relative efficiency high-purity germanium (HPGe) detector, with data collection occurring during each bremsstrahlung pulse. Total collection times varied from 4 to 8 hours, depending on the atomic number of the target. In general, the lower-Z materials produced a more attractive signal-to-noise ratio. Overall, these experiments were quite successful, particularly for the non-nuclear material targets. Clearly discernable NRF lines were identified for each of the non-nuclear targets, with definite promise being shown from the detection of the 2245 keV NRF line from ^{238}U (depleted uranium target). At the conclusion of this test series, areas of improvement for subsequent experimentation were identified: (a) increased accelerator repetition rate up to 1 kHz, (b) improved precision of accelerator electron energy resolution, and (c) optimization of detection system performance, including background reduction, detector shielding, and photon filtering.

To begin the next series of experimentation (referred to as Phase II), an additional Idaho Accelerator Center LINAC was identified and modified to produce a 1 kHz, pulsed bremsstrahlung beam. Modifications performed with this nominal 18 MeV accelerator were similar to those described above (for 600 Hz operation). Electrons from this accelerator impinged upon a 4.2 g cm^{-2} tungsten converter to produce a 1 kHz, pulsed bremsstrahlung beam, which irradiated non-nuclear and nuclear materials. Initially, a target composed of aluminum (25 mm) and boron (6 mm) was irradiated with a 3.0 MeV endpoint energy bremsstrahlung beam to assess the reproducibility of the previous 600 Hz NRF data. The NRF-produced photons were collected with a 120% relative efficiency HPGe detector, with data collection occurring during each bremsstrahlung pulse. Total collection times varied from 3 to 10 hours. While particular NRF lines were identifiable, a significant shift of the NRF lines occurred during this data collection. This was most noticeable from the separation of the 511 keV peak, which is used for energy calibration, into two distinct peaks. This peak shift was attributed to interference occurring within the detector electronics and was alleviated during data analysis. Once gain stabilization was performed, the subsequent data set showed clearly identifiable NRF lines from both the aluminum and boron in the target. The depleted uranium target, which was also irradiated with 3.0 MeV endpoint energy bremsstrahlung, produced several promising NRF lines, particularly at 2410 and 2468 keV. Follow-on tests with the same target appeared to produce similar NRF lines with an additional energy shift that continues to be investigated.

In conclusion, two individual pulsed LINACs were identified and subsequently modified to operate at 600 and 1000 Hz. Initial NRF measurements were performed on several non-nuclear targets with both low and high atomic numbers. The NRF measurements performed with a nuclear material (depleted uranium) produced promising results, although further acquisition development and detection optimization is needed. Based on FY 2008 experimental results, a clear path forward has been developed to further increase accelerator repetition rates, assess more target material configurations, and refine the data acquisition methods.

CONTENTS

SUMMARY iii

ACRONYMS viii

1. INTRODUCTION 1

2. BACKGROUND 2

3. PHASE I EXPERIMENTAL CAMPAIGN 3
   - 3.1 Experimental Setup 3
   - 3.2 Data Acquisition 4
   - 3.3 Accelerator Modifications 5
   - 3.4 Experimental Results—600 Hz 5
     - 3.4.1 Boron Measurements 6
     - 3.4.2 Aluminum Measurements 7
     - 3.4.3 Carbon (Graphite) Measurements 8
     - 3.4.4 Lead Measurements 9
     - 3.4.5 Uranium Measurements 10

4. PHASE II EXPERIMENTAL CAMPAIGN 11
   - 4.1 Experimental Setup 11
   - 4.2 Data Acquisition 12
   - 4.3 Accelerator Modifications 12
   - 4.4 Experimental Results–1 kHz 13
     - 4.4.1 Aluminum and Boron Measurements 13
     - 4.4.2 Uranium Measurements 14

5. EXPENDITURES 16

6. CONCLUSIONS 17

7. REFERENCES 18

FIGURES

Figure 1. Schematic representation of the experimental setup used in the Phase I NRF measurements. 3

Figure 2. Detector 1 shielding configuration with one side removed to show the custom Pb collimator. 4

Figure 3. Schematic representation of electronics configuration for Detector 1. 5

Figure 4. Full energy spectrum for the 50-mm Borax target, irradiated with 5.3 MeV endpoint energy bremsstrahlung (600 Hz). 6

Figure 5. ^{11}B NRF lines from the 50-mm Borax target, irradiated with 5.3 MeV endpoint energy bremsstrahlung (600 Hz). 6

Figure 6. Full energy spectrum for the 25-mm aluminum target, irradiated with 5.3 MeV endpoint energy bremsstrahlung (600 Hz). 7

Figure 7. ^{27}Al NRF lines from the 25-mm aluminum target, irradiated with 5.3 MeV endpoint energy bremsstrahlung (600 Hz). 7

Figure 8. Full energy spectrum for the 50-mm graphite target, irradiated with 5.3 MeV endpoint energy bremsstrahlung (600 Hz). 8

Figure 9. ^{12}C and ^{13}C NRF lines from the 50-mm graphite target, irradiated with 5.3 MeV endpoint energy bremsstrahlung (600 Hz). Single and double escape peaks are also highlighted. 8

Figure 10. Full energy spectrum for the 3.1-mm lead target, irradiated with 5.3 MeV endpoint energy bremsstrahlung (600 Hz). 9

Figure 11. ^{207}Pb and ^{208}Pb NRF lines from the 3.1-mm lead target, irradiated with 5.3 MeV endpoint energy bremsstrahlung (600 Hz). 9

Figure 12. Full energy spectrum for the 25-mm depleted uranium target, irradiated with 3.3 MeV endpoint energy bremsstrahlung (600 Hz). 10

Figure 13. ^{238}U NRF line from the 25-mm depleted uranium target, irradiated with 3.3 MeV endpoint energy bremsstrahlung (600 Hz). 10

Figure 14. Schematic representation of the experimental setup used in the Phase II NRF measurements. 11

Figure 15. Schematic representation of the electronics configuration for data acquisition. 12

Figure 16. Shifted 511 keV peaks prior to stabilization for the combined aluminum (25 mm) and boron (6 mm) target, irradiated with 3.0 MeV endpoint energy bremsstrahlung (1 kHz). Following application of the gain stabilization software, the 511 keV peaks are combined into one peak. 13

Figure 17. ^{27}Al (2211 keV) and ^{11}B (2124 keV) NRF lines from the combined aluminum (25 mm) and boron (6 mm) target, irradiated with 3.0 MeV endpoint energy bremsstrahlung (1 kHz). The black data represent the data prior to stabilization, while the blue data show the NRF peaks following application of the stabilization software. 14

Figure 18. Full energy spectrum for the 25-mm depleted uranium target, irradiated with 3.0 MeV endpoint energy bremsstrahlung (1 kHz). 14

Figure 19. ^{238}U NRF lines from the 25-mm depleted uranium target, irradiated with 3.0 MeV endpoint energy bremsstrahlung (1 kHz). 15
Figure 20. Graph of combined planned and actual monthly expenditures by INL and Idaho Accelerator Center. 16

TABLES

Table 1. Monthly breakdown of experimental versus monthly expenditures 16

ACRONYMS

ADC	analog-to-digital converter
HPGe	high-purity germanium
INL	Idaho National Laboratory
LINAC	linear electron accelerator
NRF	nuclear resonance fluorescence
PFN	pulse forming network
RF	radio frequency

High Repetition Rate, LINAC-Based Nuclear Resonance Fluorescence

FY 2008 Final Report

1. INTRODUCTION

This report summarizes the first year of a multi-laboratory/university, multi-year effort focusing on high repetition rate, pulsed LINAC-based nuclear resonance fluorescence (NRF) measurements. Specifically, this FY 2008 effort centered on experimentally assessing NRF measurements using pulsed linear electron accelerators (LINACs), operated at various repetition rates, and identifying specific detection requirements to optimize such measurements. Traditionally, interest in NRF as a detection technology, which continues to receive funding from the Department of Homeland Security and the Department of Energy Office of Nonproliferation and National Security (DOE/NA-22), has been driven by continuous-wave, Van de Graff-based bremsstrahlung sources. However, in addition to the relatively sparse present-day use of Van de Graff sources with electron acceleration columns, only limited NRF data from special nuclear materials has been presented; even less data are available regarding shielding effects and photon source optimization for NRF measurements on selected nuclear materials.

Any active inspection system intended for general implementation must possess sensitivity and specificity regarding materials of interest, to include special nuclear material, explosives, or other contraband. Many of the current inspection systems which use conventional x-rays, including high-energy gamma-ray imagers, do not necessarily have the ability to differentiate nuclear materials from other nonthreatening high-Z materials. Passive detection systems, many of which can provide isotope identification through the detection of unique gamma-ray and neutron signatures, lack the sensitivity to detect and identify highly shielded materials. Hence, NRF, using electron accelerator-based gamma-ray signatures, has been suggested as a method to provide sensitivity and isotope specificity for nuclear material detection and identification in many types of commercial configurations. Current interests in using NRF as a detection technology has been, in large part, driven by data produced from Passport Systems, Inc. [1,2]. Passport Systems are continuing efforts to measure resonances up to 5 MeV in ^{235}U as part of research funded by the Department of Homeland Security and DOE/NA-22. These measurements are produced with a continuous-wave Van de Graff-based bremsstrahlung source; alternative sources, such as the IBA Rhototron, are also being considered. In any case, only limited NRF data from special nuclear material has been presented at selective conferences.

This collaborative effort between Idaho National Laboratory (INL), Pacific Northwest National Laboratory, and the Idaho State University's Idaho Accelerator Center has begun to advance the understanding and application of conventional, commercially available, LINACs to NRF measurements. Initial FY 2008 research, which focused on near-term, onsite accelerator use, identified and modified an existing electron accelerator to support initial experimentation for up to 600 Hz operations. Furthermore, this work began to examine experimental configurations for optimal NRF measurements and testing with non-nuclear materials, including natural lead, aluminum, graphite (carbon), and Borax (boron). Building on initial FY 2008 efforts, a second existing LINAC was identified and modified to support higher-repetition rate operations up to 1 kHz. With this increased repetition rate capability, reproducibility assessments were performed with selected non-nuclear materials, followed by an experimental assessment of NRF measurements on nuclear material (depleted uranium) performed with a 1 kHz, pulsed LINAC.

2. BACKGROUND

The development of technology to both detect and identify shielded nuclear material is an increasingly important component of many U.S. government agencies' research efforts and mission needs. INL, in conjunction with Idaho State University's Idaho Accelerator Center, has developed extensive expertise in the area of accelerator-based active interrogation technology development and has maintained a collaborative accelerator-based detection effort for nearly two decades [3]. This expertise has been exploited to develop several novel applications supporting various governmental agencies, including the Department of Energy's Office of Nonproliferation and National Security (NA-22) and the Department of Homeland Security Domestic Nuclear Detection Office (DNDO). INL has been using gamma-ray emissions to detect nuclear materials and provide elemental specificity of explosive materials for over a decade [4–7]. INL developed the first transportable, high-energy electron accelerator system (i.e., the Varitron) in 1994 [8], which is still in use today. This system, which uses the Varitron with electron energies up to approximately 13 MeV, has demonstrated its efficiency in detecting shielded nuclear material with a novel, patented neutron detection system [3]. In addition, INL and the Idaho Accelerator Center have developed several active inspection techniques that focus on detecting and using unique radiation signatures from nuclear material. These techniques constitute a wide spectrum of identifiable signatures, including a patent-pending technique based on the time-dependence of delayed neutron emission [9, 10]. Other photonuclear inspection techniques have demonstrated the detection of 100 kg of explosives concealed within a vehicle at standoff detection distances up to 3 meters [7]. Shielded nuclear material has been detected using INL's Pulsed Photonuclear Assessment method at standoff distances exceeding 100 meters, while outdoor testing is quickly expanding standoff detection capabilities [4, 11–13].

The NRF process can occur in all nuclei with atomic numbers (Z) greater than helium (Z=2), as these nuclei possess unique and well-defined nuclear states that exist several MeV above their respective ground states [1, 2]. Population of these excited states following absorption of specific-energy photons will result in the emission of discrete energy photons (fluorescence). By using a continuous energy photon spectrum, such as accelerator-produced bremsstrahlung radiation, theses states can be readily exploited. Furthermore, since these energy states are unique from isotope to isotope, the NRF states for an individual nucleus are also unique to that isotope. Hence, NRF is a viable technique to specifically identify individual isotopes. In terms of fissionable materials of interest, there are several known resonances from ^{238}U; however, only limited data regarding NRF states in key weapon isotopes are available. While simulations have been performed, NRF responses for ^{238}U and ^{232}Th, and other nuclear materials, need to be experimentally verified in configurations comparable with an active interrogation environment. In order for NRF to be reasonably applied to an active interrogation technique, the fundamental responses of fissionable material need to be measured and the interrogating source must be optimized.

3. PHASE I EXPERIMENTAL CAMPAIGN

The focus of this first phase (Phase I) of experiments was to measure NRF transitions in non-nuclear (nonfissionable) materials. The nonfissionable targets consisted of natural lead (3.1 mm), aluminum (25 mm), graphite (50 mm), and boron (50 mm). These targets had NRF transitions that produced characteristic photons with energies ranging from approximately 2.1 to 5.5 MeV, which encompasses energies of interest for fissionable materials of interest. Furthermore, these targets provided a range of NRF transition strengths (i.e., integrated cross sections) and background characteristics due to the variations in the targets' atomic numbers. In addition to the non-nuclear materials, the team was also able to perform preliminary measurements of NRF transitions in ^{238}U (depleted uranium).

3.1 Experimental Setup

Phase I experiments were performed using the nominal 25 MeV pulsed, LINAC at the Idaho Accelerator Center. A schematic of the experimental setup is shown in Figure 1.

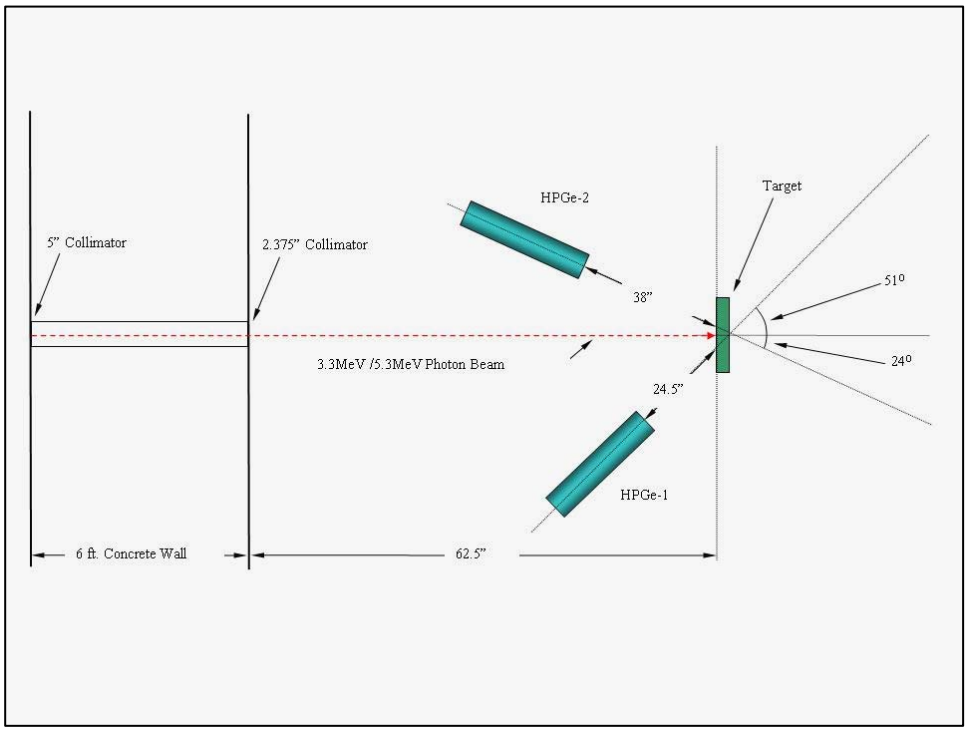

Figure 1. Schematic representation of the experimental setup used in the Phase I NRF measurements.

The LINAC produced a 3.3, 5.3, or 6.0 MeV electron beam, which impinged upon a 4.2 g cm^{-2} tungsten electron to photon converter to produce a pulsed, 600 Hz bremsstrahlung photon beam. The resulting photon beam was collimated through a 1.8-m wall into a well-shielded experimental cell. A 1.27-cm-diameter collimator was located on the accelerator hall side, followed by a 6-cm-diameter collimator located on the experimental cell side. The photon beam emerging into the experimental cell had a diameter of approximately 6.9 cm. The target was positioned 1.6 m from the experimental cell collimator. Two mechanically cooled high-purity germanium (HPGe) detectors with relative efficiencies of 62.1% (Detector 1) and 78.2% (Detector 2) were used in the experiment. Detector 1 was placed at 51 degrees to the incident beam at a distance of 62.2 cm from the target. The detector was shielded with 15.2 cm of lead on the accelerator side and 10.2 cm of lead on the remaining sides. The face of the detector was shielded with a 2.5-cm Pb filter over an 11.4-cm-diameter collimator with a 12.7-cm depth

for the boron, carbon, and aluminum targets. For the ^{238}U target, the filter was replaced with 3.2 cm of lead while keeping the detector collimation constant. Figure 2 shows the shielding configuration for Detector 1, with one side removed to show the custom Pb collimator.

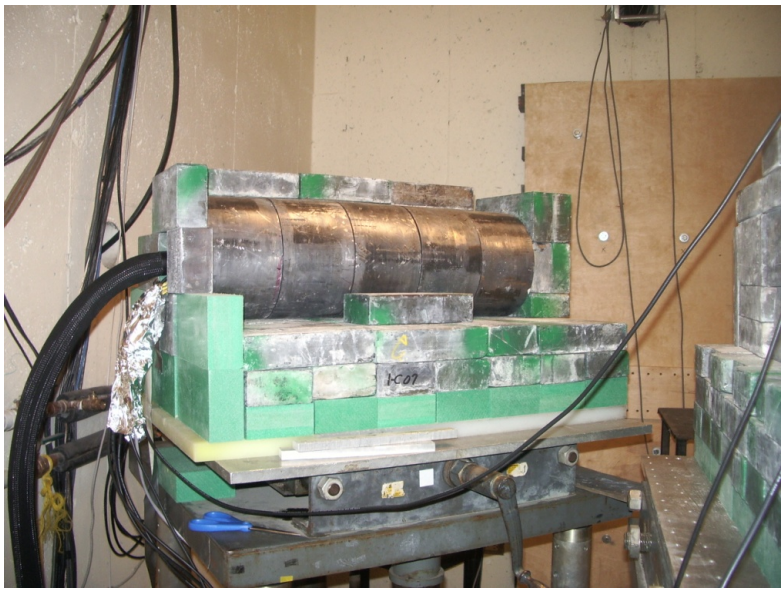

Figure 2. Detector 1 shielding configuration with one side removed to show the custom Pb collimator.

Detector 2 was placed at 24 degrees to the beam and 96.5 cm from the target. Detector 2 was collimated using a 5.1 cm × 7.6 cm square collimator, which was 20.3 cm deep and followed by a 1.9-cm thick Pb filter for all targets. The electron charge per pulse on the bremsstrahlung radiator and the thickness of the Pb absorbers in front of the detectors were adjusted to maintain a total count rate of approximately 0.1 counts per bremsstrahlung pulse in each of the detectors.

3.2 Data Acquisition

During the first experimental campaign, the output signal from Detector 1 was processed through two separate electronic configurations. Configuration 1 had the HPGe output sent into an amplifier, followed by an analog-to-digital converter (ADC). A timing pulse from the accelerator electron gun trigger was also sent to the ADC, ensuring data were only collected during the bremsstrahlung pulse. The output for Configuration 2 was passed to a similar amplifier and ADC; however, data collection occurred continuously. Figure 3 is a schematic representation of the electronics configuration for Detector 1. The timing pulse from the accelerator electron gun pulse was also sent to an additional ADC and then to the acquisition software. This provided a temporal reference point for the collected data, which allowed a timing gate, similar to Output 1, to be applied to the Output 2 data following data collection as part of the data analysis.

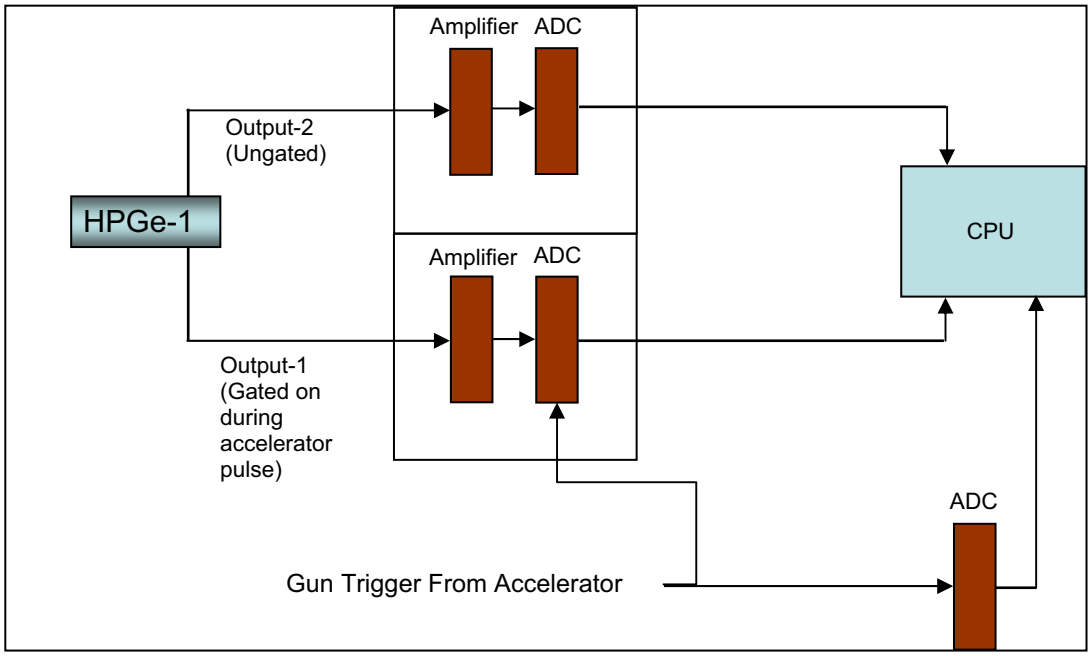

Figure 3. Schematic representation of electronics configuration for Detector 1.

3.3 Accelerator Modifications

To facilitate the high repetition rate, LINAC-based NRF measurements, the 25 MeV electron accelerator at the Idaho Accelerator Center was modified to increase the maximum operable repetition rate from 300 Hz up to 600 Hz. The first step in increasing the maximum repetition rate was a reduction in the total capacitance and inductance of the pulse forming network (PFN). Essentially, the PFN is a series of capacitors and inductors that stores the high voltage provided by a power supply. Once the PFN is charged, the thyratron, which acts as a power-regulation switch, causes the power stored in the PFN to discharge into the klystron (radio frequency [RF] source). As the total charging time is governed by the total capacitance and inductance of the PFN, reducing the number of components within the PFN results in a shorter charge time and decreased power pulse width. Specifically, three of the six capacitors and three of the six inductors were effectively removed from the PFN charging circuit, resulting in a 3 μs wide power pulse supplied to the klystron. The pulse width provided to the klystron by the radio frequency driver was set to approximately 6 μs. Therefore, the total pulse width of the radio frequency pulse, which is subsequently injected into the accelerator waveguide to accelerate the electrons, was minimized to 3 μs.

Two final modifications were applied, with the addition of an alternative thyratron and an increase in the PFN charging power provided by the external power supply. As mentioned above, the thyratron acts as the switch for the discharging process of the PFN. As a result, as much as 50% of the total power released from the PFN is dropped into the thyratron. Prior to the modifications, this accelerator contained a glass thyratron. Because an increased amount of power (up to 12 kW) was needed to decrease the total PFN charging time for each pulse, it was predicted that the glass thyratron would experience some difficulties operating with the increased power. Hence, it was replaced with a ceramic thyratron that is more suitable for the higher-power operations.

3.4 Experimental Results—600 Hz

This section provides non-nuclear and nuclear NRF results of the Phase I experimental campaign.

3.4.1 Boron Measurements

Figure 4 shows the full energy spectrum for the boron target. Specifically, this target was a 50-mm-thick borax target, irradiated with 5.3 MeV endpoint energy bremsstrahlung (600 Hz). Figure 5 shows a selected region of the full energy spectrum with the NRF lines of interest highlighted. The 2124, 4445, and 5022 keV lines are all characteristic of the ^{11}B isotope.

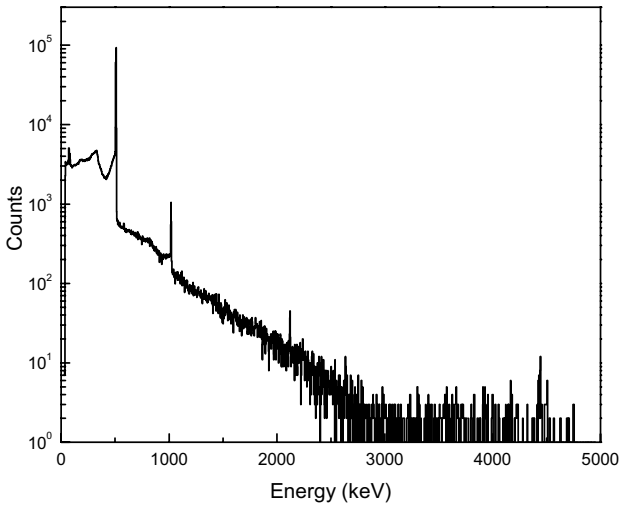

Figure 4. Full energy spectrum for the 50-mm Borax target, irradiated with 5.3 MeV endpoint energy bremsstrahlung (600 Hz).

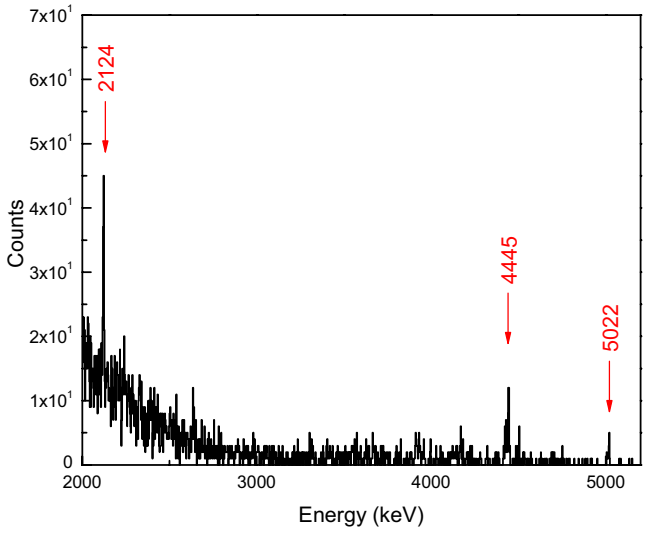

Figure 5. ^{11}B NRF lines from the 50-mm Borax target, irradiated with 5.3 MeV endpoint energy bremsstrahlung (600 Hz).

3.4.2 Aluminum Measurements

Figure 6 shows the full energy spectrum for the 25-mm-thick aluminum target, irradiated with 5.3 MeV endpoint energy bremsstrahlung (600 Hz). Figure 7 shows a selected region of the full energy spectrum with the NRF lines of interest highlighted. The 2211, 2981, and 3957 keV lines are each from the ^{27}Al isotope.

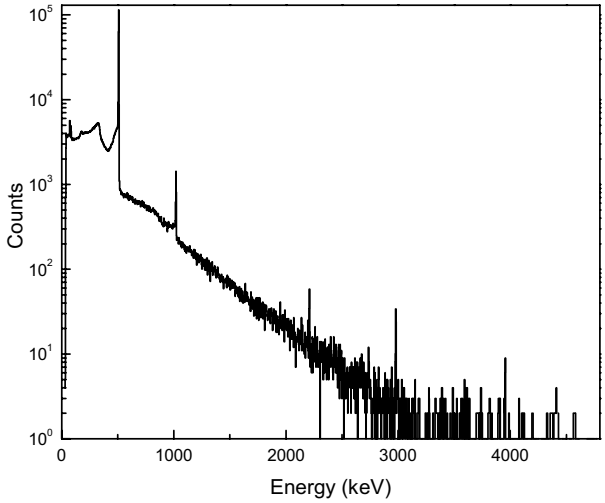

Figure 6. Full energy spectrum for the 25-mm aluminum target, irradiated with 5.3 MeV endpoint energy bremsstrahlung (600 Hz).

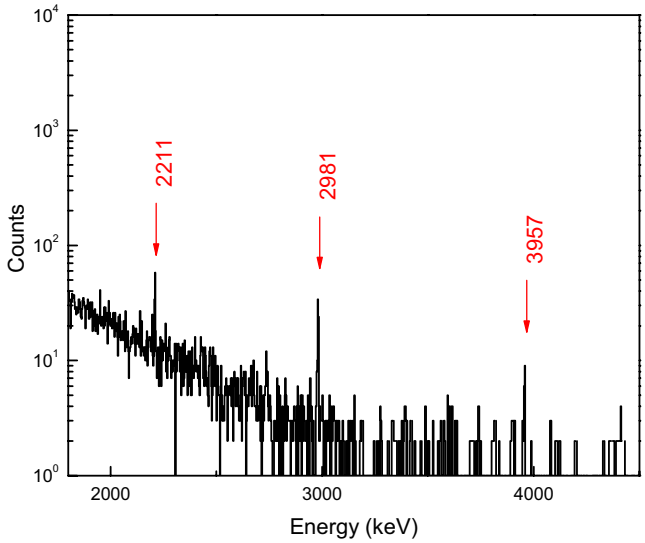

Figure 7. ^{27}Al NRF lines from the 25-mm aluminum target, irradiated with 5.3 MeV endpoint energy bremsstrahlung (600 Hz).

3.4.3 Carbon (Graphite) Measurements

Figure 8 shows the full energy spectrum for the 50-mm-thick graphite target, irradiated with 5.3 MeV endpoint energy bremsstrahlung (600 Hz). Figure 9 shows a selected region of the full energy spectrum with the NRF lines of interest highlighted. The 3089 and 3684 keV lines are from ^{13}C, while the 4438 keV line is characteristic of ^{12}C.

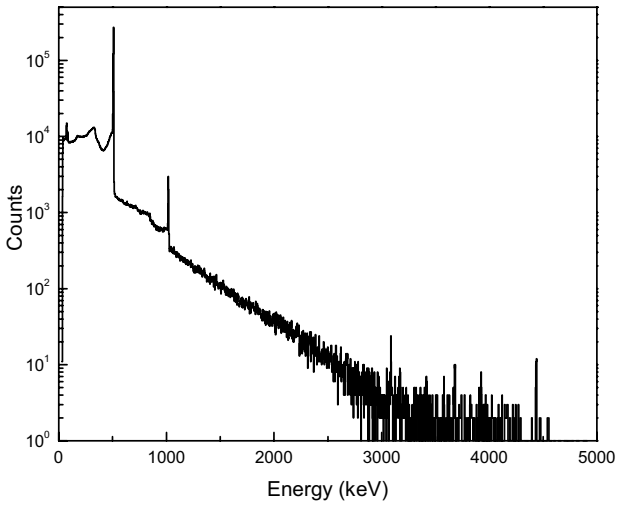

Figure 8. Full energy spectrum for the 50-mm graphite target, irradiated with 5.3 MeV endpoint energy bremsstrahlung (600 Hz).

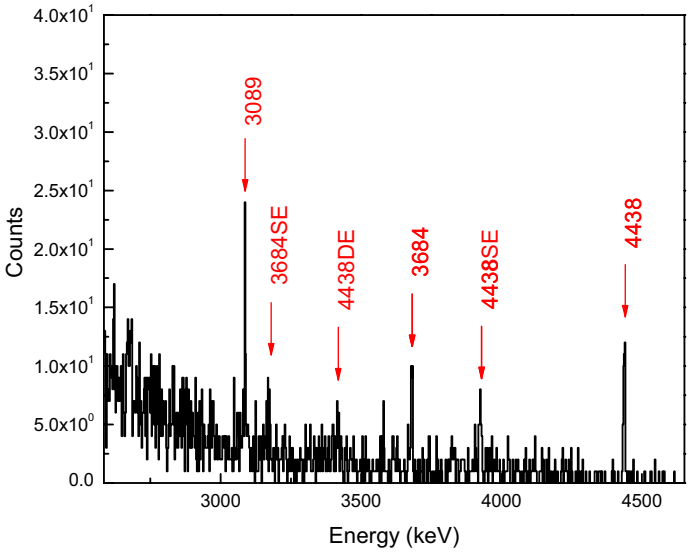

Figure 9. ^{12}C and ^{13}C NRF lines from the 50-mm graphite target, irradiated with 5.3 MeV endpoint energy bremsstrahlung (600 Hz). Single and double escape peaks are also highlighted.

3.4.4 Lead Measurements

Figure 10 shows the full energy spectrum for the 3.1-mm-thick natural lead target, irradiated with 5.3 MeV endpoint energy bremsstrahlung (600 Hz). Figure 11 shows a selected region of the full energy spectrum with the NRF lines of interest highlighted. The 4140 keV line is from ^{207}Pb, while the 4842 keV line is characteristic of ^{208}Pb.

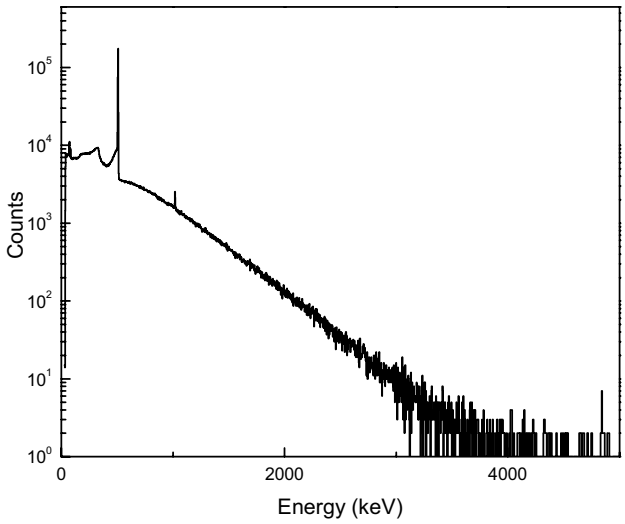

Figure 10. Full energy spectrum for the 3.1-mm lead target, irradiated with 5.3 MeV endpoint energy bremsstrahlung (600 Hz).

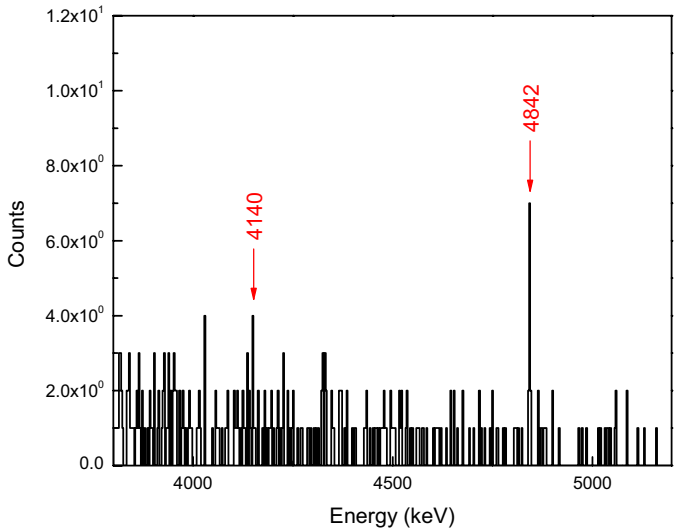

Figure 11. ^{207}Pb and ^{208}Pb NRF lines from the 3.1-mm lead target, irradiated with 5.3 MeV endpoint energy bremsstrahlung (600 Hz).

3.4.5 Uranium Measurements

Figure 12 shows the full energy spectrum for the 25-mm-thick depleted uranium target, irradiated with 3.3 MeV endpoint energy bremsstrahlung (600 Hz). Figure 13 shows a selected region of the full energy spectrum with the NRF lines of interest highlighted. The 2245 keV line is characteristic of ^{238}U.

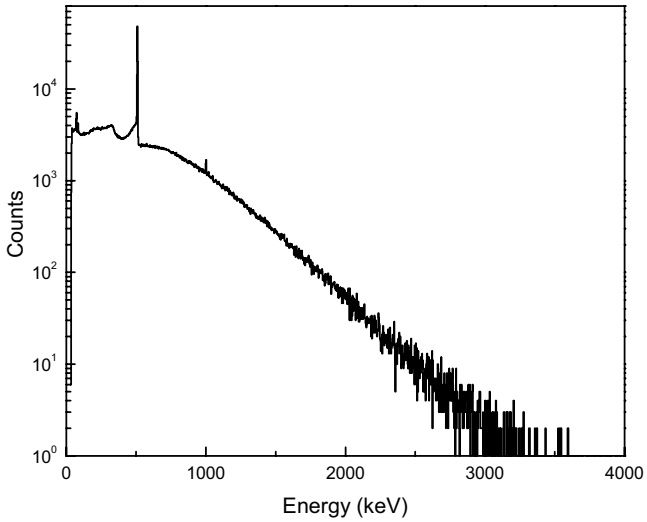

Figure 12. Full energy spectrum for the 25-mm depleted uranium target, irradiated with 3.3 MeV endpoint energy bremsstrahlung (600 Hz).

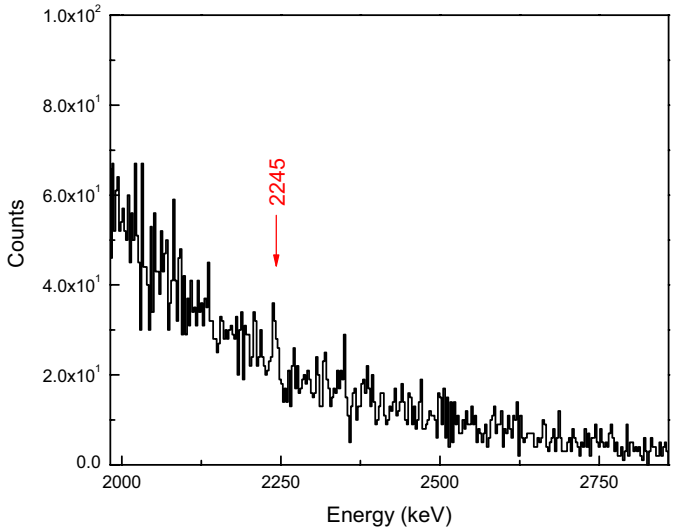

Figure 13. ^{238}U NRF line from the 25-mm depleted uranium target, irradiated with 3.3 MeV endpoint energy bremsstrahlung (600 Hz).

4. PHASE II EXPERIMENTAL CAMPAIGN

The focus of the second phase of experiments was to measure NRF transitions in both non-nuclear and nuclear materials at an increased accelerator repetition rate. The non-nuclear target was a combination of aluminum (25 mm) and boron (6 mm), while the nuclear target was a 25-mm depleted uranium plate. For this phase, an additional pulsed, electron LINAC was identified and modified to produce a pulsed bremsstrahlung beam with a repetition rate up to 1 kHz.

4.1 Experimental Setup

The Phase II experiments were performed using an 18 MeV pulsed electron linear accelerator at the Idaho Accelerator Center's campus facility. A schematic of the experimental setup is shown in Figure 14.

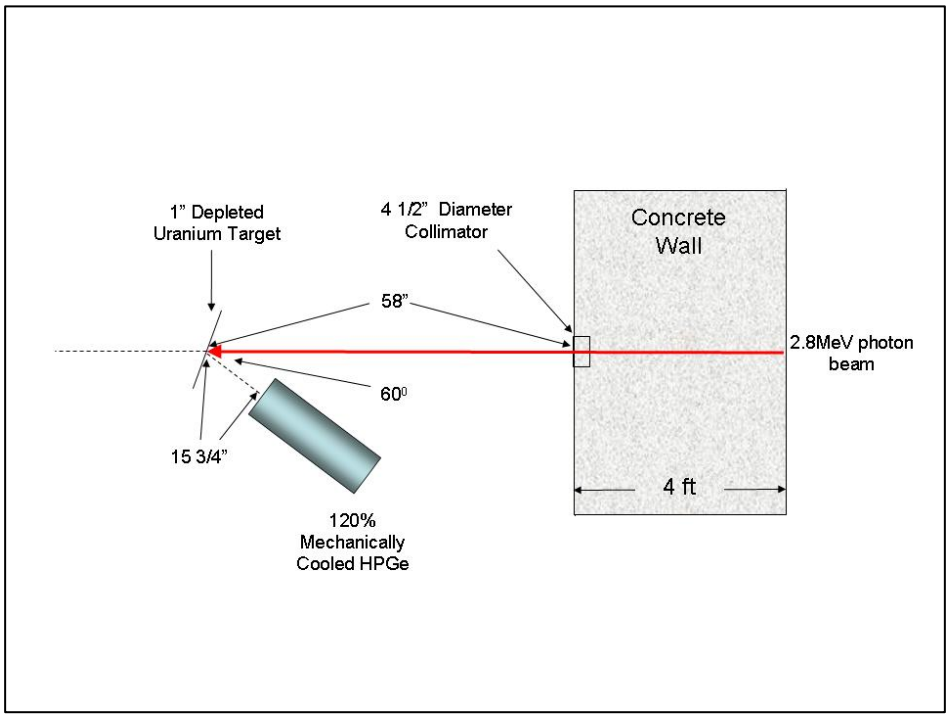

Figure 14. Schematic representation of the experimental setup used in the Phase II NRF measurements.

The electron LINAC was used to produce a 2.7, 2.8, or 3.0 MeV electron beam incident on a 4.2 g cm^{-2} tungsten converter to produce a 1 kHz pulsed bremsstrahlung photon beam. The charge on converter was kept to the maximum available charge of approximately 5 nC per pulse. The resulting beam was collimated through a 1.2-m concrete wall into a shielded area of the accelerator hall. Collimation consisted of a 1-cm diameter Pb collimator on the wall closest to the accelerator and an 11.5-cm-diameter collimator on the wall closest to the target. The collimator on the wall closest to the accelerator was primarily responsible for and dominated the collimation effect. The tungsten converter was placed 150 cm from the accelerator collimator, resulting in an approximately 4-cm-diameter beam spot at the target. A mechanically cooled HPGe detector with a relative efficiency of 120% was placed 41 cm from the target and at an angle of 60 degrees to the photon beam. The HPGe detector was shielded with approximately 15 cm of Pb, including the cylindrical collimator shown in Figure 2. The face of the detector was collimated to an 11.4-cm-diameter opening with a 10-cm depth. A sheet of Pb, ranging in thickness from 2 cm to 2.5 cm, was placed over the face of the detector to filter out low energy γ-rays. The thickness of Pb over the face of the detector was varied to maintain a count rate of 0.1 counts per accelerator pulse.

Because of excess radio frequency noise generated by the accelerator flash, a gain shift in the resulting spectra was observed. To compensate for the gain shift, gain stabilization software was used to realign the spectra. The 511-keV peak was used as a basis for stabilization because it forms very quickly and is visible quickly in the data acquisition period.

4.2 Data Acquisition

During the second experimental campaign, the output signal from the HPGe was sent into an amplifier, followed by an ADC. A timing pulse from the accelerator electron gun trigger was also sent to the ADC, ensuring data were only collected during the bremsstrahlung pulse. Figure 15 is a schematic representation of the electronics configuration for Detector 1. The timing pulse from the accelerator electron gun pulse was also sent to an additional ADC and then to the acquisition software. This provided a temporal reference point for the collected data, which allowed a timing gate to be manually applied to the data following data collection as part of the data analysis.

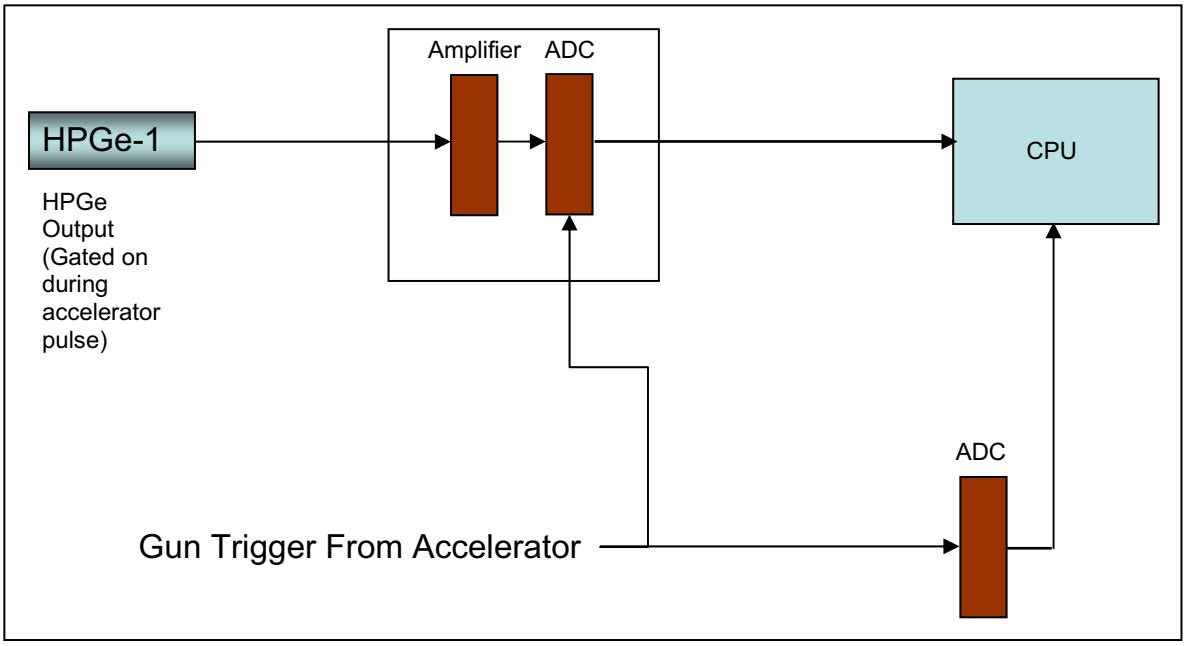

Figure 15. Schematic representation of the electronics configuration for data acquisition.

4.3 Accelerator Modifications

The first modification performed on the LINAC utilized for the second experimental campaign was the replacement of the accelerating waveguide. Once installed, the new waveguide allowed for a maximum electron energy of approximately 18 MeV and a minimum energy of approximately 2.5 MeV. All additional modifications were similar to those described in Section 3.3.

4.4 Experimental Results–1 kHz

This section provides non-nuclear and nuclear NRF results of the Phase II experimental campaign.

4.4.1 Aluminum and Boron Measurements

Initially, a combined aluminum (25 mm) and boron (6 mm) target was irradiated with 3.0 MeV endpoint energy bremsstrahlung (1 kHz) as a reproducibility assessment. During the course of this measurement, a significant shift in the peak locations occurred. This was most noticeable in the formation of two separate 511 keV peaks. It was determined that this shift was a result of excess radio frequency noise generated by the accelerator pulse producing interference in the gain on the HPGe electronics. Consequently, to compensate for the gain shift, gain stabilization software was written and used to realign the spectra. Because the 511 keV peak is generated very quickly and is visible in a short time period, this peak was served as the basis for stabilization. Figure 16 shows the two shifted 511 keV peaks prior to stabilization and the combined peak following application of the stabilization software. Once stabilization was achieved, the NRF lines of interest were clearly visible, as can be seen in Figure 17.

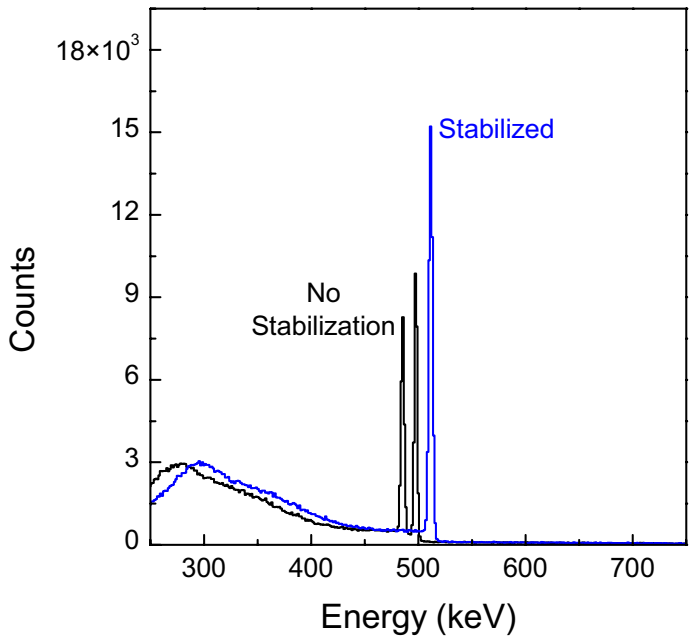

Figure 16. Shifted 511 keV peaks prior to stabilization for the combined aluminum (25 mm) and boron (6 mm) target, irradiated with 3.0 MeV endpoint energy bremsstrahlung (1 kHz). Following application of the gain stabilization software, the 511 keV peaks are combined into one peak.

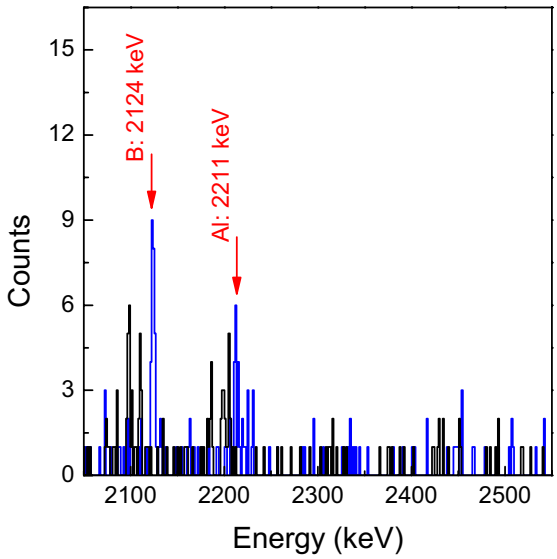

Figure 17. ^{27}Al (2211 keV) and ^{11}B (2124 keV) NRF lines from the combined aluminum (25 mm) and boron (6 mm) target, irradiated with 3.0 MeV endpoint energy bremsstrahlung (1 kHz). The black data represent the data prior to stabilization, while the blue data show the NRF peaks following application of the stabilization software.

4.4.2 Uranium Measurements

Figure 18 shows the full energy spectrum for the 25-mm-thick depleted uranium target, irradiated with 3.0-MeV endpoint energy bremsstrahlung (1 kHz). Figure 19 shows a selected region of the full energy spectrum with the NRF lines of interest highlighted. All highlighted lines are characteristic of ^{238}U.

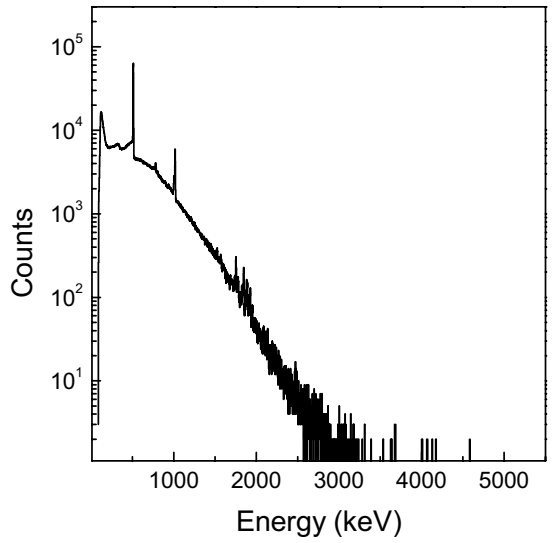

Figure 18. Full energy spectrum for the 25-mm depleted uranium target, irradiated with 3.0 MeV endpoint energy bremsstrahlung (1 kHz).

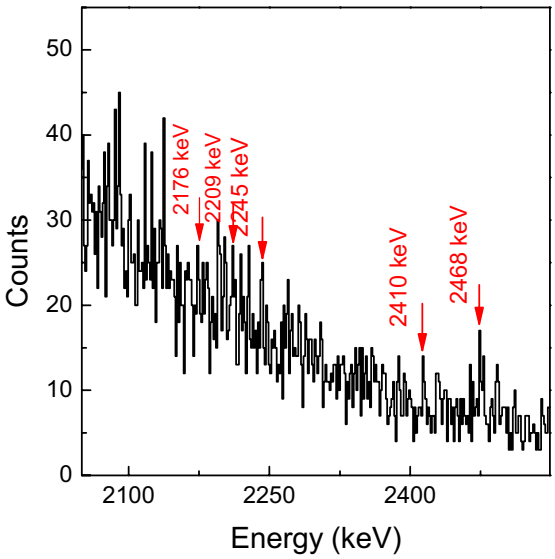

Figure 19. ^{238}U NRF lines from the 25-mm depleted uranium target, irradiated with 3.0 MeV endpoint energy bremsstrahlung (1 kHz).

5. EXPENDITURES

A total of $525,000 was funded and budgeted for the FY 2008 effort. A contract was written to the Idaho Accelerator Center for $200,000 to accommodate accelerator modifications and to fund needed engineering labor as well as scientific collaboration. Figure 20 and Table 1 show the monthly expenditures by both the INL and the Idaho Accelerator Center combined.

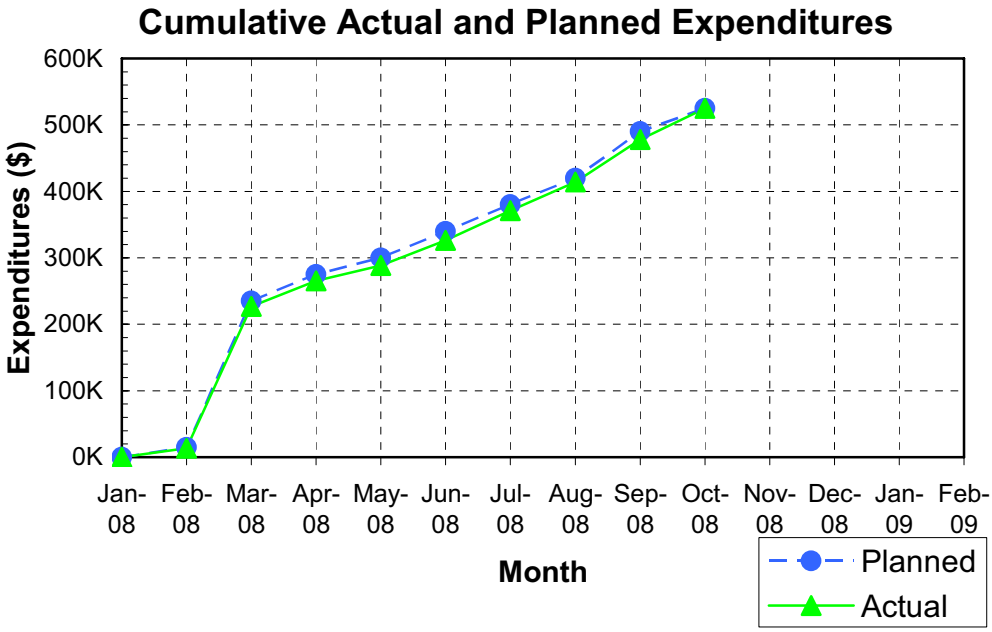

Figure 20. Graph of combined planned and actual monthly expenditures by INL and Idaho Accelerator Center.

Table 1. Monthly breakdown of experimental versus monthly expenditures.

Phase	Date	Actual in Period ($)	Cumulative Actual	Planned for Period ($)	Cumulative Planned
1	1/1/2008	0	0	0	0
1	2/1/2008	13,494	13,494	15000	15,000
1	3/3/2008	213,614	227,108	220000	235,000
1	4/2/2008	38,544	265,652	40000	275,000
1	5/3/2008	23,002	288,654	25000	300,000
2	6/3/2008	37,728	326,382	40000	340,000
2	7/3/2008	44,797	371,179	40000	380,000
2	8/3/2008	43,276	414,455	40000	420,000
2	9/2/2008	63,500	477,955	70000	490,000
2	10/2/2008	47,045	525,000	35000	525,000

6. CONCLUSIONS

The FY 2008 effort focused on using a variable repetition rate, pulsed LINAC to experimentally assess NRF measurements. Included in the effort was the identification of specific detection necessities and requirements for the optimization of these measurements. An existing nominal 25 MeV electron accelerator, located at the Idaho Accelerator Center, was modified to increase the previous repetition rate of 300 Hz up to 600 Hz. The capacitance and inductance of the PFN was minimized to reduce its effective charging and discharging time, resulting in a total PFN power pulse width of 3 μs. The radio frequency driver pulse width was also reduced to approximately 6 μs, which, in combination with the PFN modifications, enabled a total radio frequency pulse width of 3 μs. To further enable an increase in the system's repetition rate, the PFN charging power was increased up to 12 kW, which required an additional system modification in the form of replacing the existing glass thyratron with a ceramic thyratron.

In order to optimize the experimental setup and perform baseline testing with non-nuclear materials, a series of preliminary experiments was performed for NRF-type measurements with a repetition rate up to 600 Hz. The modified electron LINAC was tuned to produce 3.3 and 5.3 MeV electrons, which interacted within a 4.2 $g \cdot cm^{-2}$ tungsten electron to photon converter, resulting in a 600 Hz, pulsed bremsstrahlung beam. Preliminary measurements were then performed on several non-nuclear targets, including ^{nat}Pb (3.1 mm), ^{27}Al (25 mm), graphite (50 mm), and Borax (50 mm), where each was irradiated with 5.3 MeV endpoint energy bremsstrahlung. An initial series of measurements was also collected with nuclear material, in the form of a 25-mm-thick depleted uranium target. A 62.1% relative efficiency HPGe detector collected the NRF-produced photons, which were detected during each accelerator pulse for collection times ranging from 4 to 8 hours. This phase of experimentation was quite successful, especially in regard to the non-nuclear material targets, with the lower-Z materials producing increased signal-to-noise ratios. The depleted uranium target also showed promising results via the identification of the 2245 keV photon line from ^{238}U.

Following the initial measurements, an additional Idaho Accelerator Center LINAC, located at Idaho State University, was modified to operate with a repetition rate up to 1 kHz. This nominal 18 MeV accelerator was modified in the same manner as the 600-Hz LINAC and was used to produce a 1 kHz, pulsed bremsstrahlung beam. To assess the reproducibility of the NRF measurements performed at 600 Hz, a target combining aluminum and boron was irradiated with 3.0 MeV endpoint energy bremsstrahlung, while a 120% relative efficiency HPGe detector was used to collect the NRF-produced photons. During these measurements, an apparent shift in the NRF lines occurred, which was identifiable from the formation of two individual 511 keV peaks. This shift, which was attributed to interference within the detector's supporting electronics, was accounted for and corrected during the subsequent data analysis. Following alleviation of the peak shift, NRF lines from both the aluminum and boron were clearly discernable. Irradiation of the depleted uranium target with 3.0 MeV endpoint energy bremsstrahlung produced identifiable NRF lines, specifically at 2410 and 2468 keV (^{238}U lines). An additional data set collected from the uranium target produced similar NRF lines; however, an additional shift in the NRF lines was apparent, which is still being investigated. Total data collection times for these measurements ranged from 3 to 10 hours.

In summary, two existing pulsed LINACs were identified and modified to support NRF-type measurements at repetition rates up to 600 and 1000 Hz, respectively. Initial NRF measurements performed on several non-nuclear targets, with both low and high atomic numbers, were quite successful and produced clearly discernable NRF lines for each target. Follow-on measurements performed with nuclear material (depleted uranium) also showed promising results; however, further data acquisition development and detection optimization is recommended to include further increases in accelerator repetition rates and further individual and composite nuclear and non-nuclear material assessments.

7. REFERENCES

1. W. Bertozzi and R. J. Ledoux, "Nuclear resonance fluorescence imaging to non-intrusive cargo inspection," *Nucl. Instrum. and Methods Phys, Res., Sect. B*, **241**, 820 (2005).
2. W. Bertozzi, S. E. Korbly, R. J. Ledoux, and W. Park, "Nuclear resonance fluorescence and effective Z determination applied to detection and imaging of special nuclear material, explosives, toxic substances and contraband," *Nucl. Instrum. and Methods Phys, Res., Sect. B,* **261**, 331 (2007).
3. J. L. Jones, W. Y. Yoon, K. J. Haskell, D. R. Norman, J. M. Zabriski, J. W. Sterbentz, S, M. Watson, J. T. Johnson, B. D. Bennett, R. W. Watson, K. L. Folkman, "Pulsed Photonuclear Assessment (PPA) Technique: CY 04 Year-End Progress Report," Formal Report, INEEL/EXT-05-02583, February 2005.
4. D. R. Norman, J. L. Jones, B. W. Blackburn, K. J. Haskell, J. T. Johnson, S. M. Watson, A. W. Hunt, R. Spaulding and F. Harmon, "Time-dependent delayed signatures from energetic photon interrogations," *Nucl. Instrum. and Methods Phys, Res., Sect. B,* **261**, 316 (2007).
5. J. L. Jones, *SPIE Proceedings* **2867**, 202 (1996).
6. T. R. Twomey, A. J. Caffrey and D. L. Chichester, "Nondestructive Identification of Chemical Warfare Agents and Explosives by Neutron Generator-Driven PGNAA," INL Report, INL/CON-07-12304, February 2007.
7. "Better Than Dogs," *Need to Know*, INL National Security Newsletter **3**, 2, 6 (January 2003).
8. J. L. Jones, et al., "Pulsed Photoneutron Interrogation: The GNT Demonstration System," Formal Report, WINCO-94-1225, October 1994.
9. M. T. Kinlaw and A. W. Hunt, "Time dependence of delayed neutron emission for fissionable isotope identification," *Appl. Phys. Lett*. **86**, 254104 (2005).
10. M. T. Kinlaw and A. W. Hunt, "Fissionable isotope identification using the time dependence of delayed neutron emission," *Nucl. Instrum. and Methods Phys, Res., Sect. A***, 562**, 1081-1084 (2006).
11. J. L. Jones, W. Y. Yoon, Y. D. Harker, J. M. Hoggan, K. J. Haskell, L. A. VanAusdeln, "Proof-of-Concept Assessment of a Photofission-Based Interrogations System for Detection of Shielded Nuclear Material," INEEL/EXT-2000-01523, November 2000.
12. J. L. Jones, Daren R. Norman, Kevin J. Haskell, James W. Sterbentz, Woo Y. Yoon, Scott M. Watson, James T. Johnson, John M. Zabriskie, Brion D. Bennett, Richard W. Watson, Cavin E. Moss, J. Frank Harmon, "Detection of shielded nuclear material in a cargo container*," Nucl. Instrum. and Methods Phys, Res., Sect. A,* **562**, 1085 (2006).
13. J. L. Jones, B. W. Blackburn, S. M. Watson, D. R. Norman, and A. W. Hunt, "High-energy photon interrogation for nonproliferation applications," *Nucl. Instrum. and Methods Phys, Res., Sect. B*, **261**, 326-330 (2007).